Title

Identification of Adenosine Deaminase Inhibitors by Metal-binding Pharmacophore Screening

Journal

ChemMedChem, 15(22)

ISSN

1860-7179

Authors

Adamek, Rebecca N
Ludford, Paul
Duggan, Stephanie M
et al.

Publication Date

2020-11-18

DOI

10.1002/cmdc.202000271

Peer reviewed

HHS Public Access

Author manuscript

ChemMedChem. Author manuscript; available in PMC 2021 November 18.

Published in final edited form as:

ChemMedChem. 2020 November 18; 15(22): 2151–2156. doi:10.1002/cmdc.202000271.

Identification of Adenosine Deaminase Inhibitors by Metal-binding Pharmacophore Screening

Rebecca N. Adamek[+,a], **Paul Ludford**[+,a], **Stephanie M. Duggan**[a], **Yitzhak Tor**[a], **Seth M. Cohen**[a]

[a]Department of Chemistry and Biochemistry, University of California, San Diego, La Jolla, CA 92093 (USA)

Abstract

Adenosine deaminase (ADA) is a human mononuclear Zn^{2+} metalloenzyme that converts adenosine to inosine. ADA is a validated drug target for cancer, but there has been little recent work on the development of new therapeutics against this enzyme. The lack of new advancements can be partially attributed to an absence of suitable assays for high-throughput screening (HTS) against ADA. To facilitate more rapid drug discovery efforts for this target, an in vitro assay was developed that utilizes the enzymatic conversion of a visibly emitting adenosine analogue to the corresponding fluorescent inosine analogue by ADA, which can be monitored via fluorescence intensity changes. Utilizing this assay, a library of ~350 small molecules containing metal-binding pharmacophores (MBPs) was screened in an HTS format to identify new inhibitor scaffolds against ADA. This approach yielded a new metal-binding scaffold with a K_i value of 26±1 μM.

Graphical Abstract

scohen@ucsd.edu.

[+]These authors contributed equally to this work

Supporting information for this article is available on the WWW under https://doi.org/10.1002/cmdc.202000271

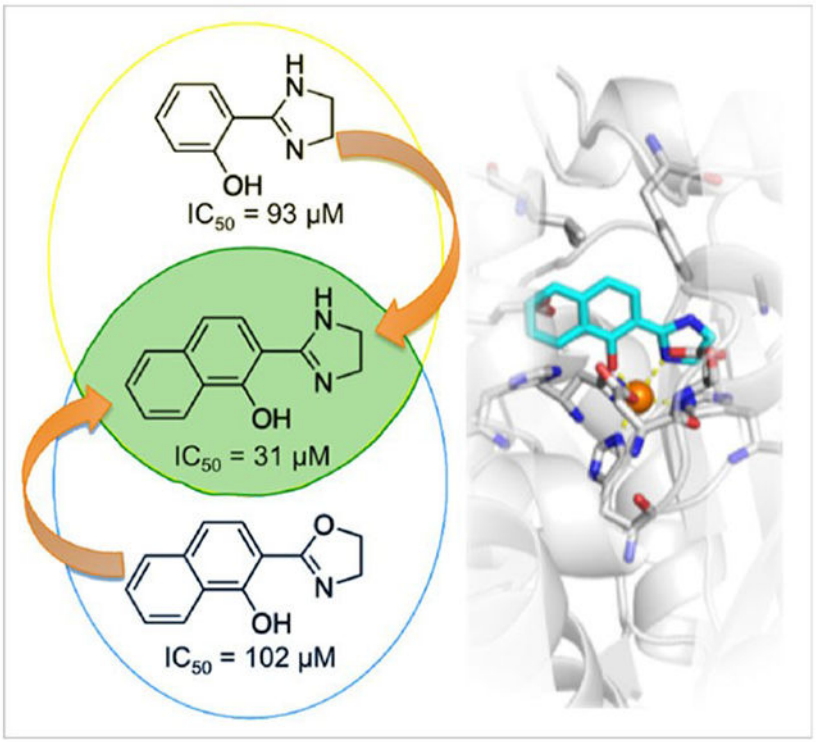

Metal-binding inhibitors of the metalloenzyme adenosine deaminase (ADA) were discovered by high-throughput screening. A fragment merge strategy of combining active scaffolds led to the discovery of an imidazoline-based inhibitor. This work demonstrates the potential of metal-binding inhibitors to provide novel routes for ADA inhibition for therapeutic intervention.

Keywords

Fluorescent Probes; Fragment Based Drug Discovery; High Throughput Screening; Medicinal Chemistry; Metalloenzymes

Introduction

Adenosine deaminase (ADA EC 3.5.4.4), also known as adenosine dehydrolyase, is found across nearly all domains of life, and plays a vital role in purine metabolism. This mononuclear Zn^{2+}-dependent metalloenzyme functions to deaminate adenosine and 2′-deoxyadenosine to yield inosine and 2′-deoxyinosine, respectively.[1]

ADA activity has been implicated in certain types of cancers, including lymphoma and leukemia.[2] As ADA has been associated with other lymphoproliferative disorders, inhibitors of ADA have been sought after as potential therapeutic agents.[3] However, considering that ADA is also necessary for immune system activity, reversible ADA inhibitors are preferable to avoid potential on-target toxicity associated with irreversible inhibitors. Currently there are only two FDA-approved ADA inhibitors, pentostatin and cladribine (Figure 1), which are both clinically used in the treatment of hairy cell leukemia.

[1a,4] Notably, the potent ADA inhibitor erythro-9-(2-hydroxy-3-nonyl) adenine (EHNA), is often used as a research tool, but failed to enter clinical trials due to poor metabolism-related pharmacokinetic properties.[4b,5] The discovery of new ADA inhibitors remains a significant challenge.[6]

Current bioaffinity methods to analyze ADA activity include chromatographic separations, [6c] which are labor and time consuming, and absorption spectroscopy, the latter of which suffers from optical interference by inhibitors that display absorption in the wavelengths between 200–300 nm, where adenosine and its derivatives absorb.[4a,6a,b,d] While newer methods have been disclosed,[7] to the best of our knowledge, their application in high-throughput screening (HTS) has not been realized. Herein, we demonstrate the use of a new HTS assay for ADA based on a recently described, fluorescent reporter of ADA activity. The method relies on isothiazolo adenosine (^{tz}A), a visibly emitting adenosine surrogate as a mimic of the native substrate.[8] This isothiazolo-based purine analog (K_M=19 μM) undergoes deamination as effectively as adenosine (K_M=28 μM) yielding ^{tz}I, the corresponding distinctly emissive inosine isostere.[7e] These easily detectable fluorescence changes serve as the foundation for a real-time and sensitive assay for the discovery of ADA inhibitors, which can be executed using commercial plate readers,[7e] thereby facilitating more rapid drug discovery efforts.

The deamination mechanism of ADA has been thoroughly investigated (Figure 1).[1a] The catalytic Zn^{2+} is coordinated by His15, His17, His214, and Asp295 with a water/hydroxide completing the distorted trigonal bipyramidal coordination geometry.[9] This Zn^{2+}-activated nucleophilic water attacks the adenosine at the C6 position, and the resulting rehybridization, involving the departure of ammonia affords inosine (Figure 1). Notably, active site amino acid side-chain residues and water molecules mediate the necessary proton transfer reactions to complete the deamination mechanism. While the majority of ADA inhibitors are adenosine surrogates or transition state analogs, the mechanism articulated above suggests that binding to the catalytic Zn^{2+} could effectively inactivate this metalloenzyme.[10] Therefore, it was decided to employ a metal-binding pharmacophore (MBP) strategy against ADA in an effort to discover new inhibitory motifs.

The use of MBPs to target the metal ion co-factor in metalloenzymes has been demonstrated to be a viable approach for inhibitor development.[10-11] One of the primary benefits of the MBP approach is the intrinsic strength of the non-covalent, reversible coordinate covalent bond, allowing for a high ligand efficiency from the MBP alone. This MBP approach is highly compatible with fragment-based drug discovery (FBDD). Herein, we utilize the previously described ^{tz}A to ^{tz}I biophysical assay[7e] in an HTS format, and use this tool to evaluate a library of ~350 MBPs in an effort to discover new, metal-binding inhibitors of ADA. Subsequent lead elaboration, as guided by structure-activity relationship (SAR) analysis, resulted in the identification of structural motifs that contributed to fragment activity, resulting in the discovery of a new imidazoline scaffold for ADA inhibitors.

Results

A library of ~350 MBPs was screened at an initial concentration of 200 μM in an HTS format, based on the ^{tz}A to ^{tz}I reaction[7e] in a 96-well plate format. Fluorescence changes were monitored following excitation at 322 nm and an emission wavelength of 410 nm. As a positive control, EHNA was screened in a 10-point inhibition curve (see Experimental part and SI; Figure S1), and was determined to have an IC_{50} value of 6±2 nM, consistent with literature values.[1a,7d,e] All MBP fragments were screened in triplicate with a positive (EHNA 10 μM) and negative (buffer only) control. From this screen, 36 MBPs were identified to have >50% ADA inhibition at 200 μM, and an additional 20 compounds had >75% ADA inhibition this concentration (Figure 2). Of these, compound **1** had the highest overall activity in the initial screen with 89% inhibition of ADA activity relative to the negative control (Figure 3). Scaffolds **2** and **3** also emerged as potential lead fragments, with activities of ~83% inhibition at 200 μM against ADA (Figure 3).

To further validate the fluorescent assay transition to a plate reader format, an IC_{50} curve for **2** was generated and gave a value of 30±1 μM (Figure S2). From this curve, the percent inhibition of ADA at 200 μM **2** was 84%, which was consistent with the value previously obtained in the initial MBP library screen; serving as a secondary control to demonstrate conversion of the assay to a HTS, plate-based format.

Oxazoline derivative synthesis and inhibitory activity

The phenol derivatives 2-imidazolyl phenol and 2-oxazolyl phenol (**3** and **4**, respectively) inhibited ADA-mediated deamination by 83% and 61%, respectively at 200 μM. Complete titrations of ADA activity with **3** and **4** yielded IC_{50} values of 93±17 and 260±14 μM, respectively (Figures S3 and S4, respectively). Although these oxazoline- and imidazoline-based compounds are known as components of certain siderophores,[12] to the best of our knowledge, they have not been widely used as metalloenzyme inhibitors. To further explore this structural motif, a total of 11 derivatives of 4 were prepared to develop a structure-activity relationship (SAR) of the oxazoline scaffold against ADA (Figure 3). Table 1 lists the IC_{50} values for these derivatives.

The synthesis of these oxazoline derivatives was straightforward (Scheme 1). Cyclization to form the oxazoline ring was achieved by heating pre-functionalized 2-hydroxybenzonitriles with ethanolamine and catalytic amounts of $ZnCl_2$ at 110°C in toluene for 16 h. Subsequent work-up gave **3–5** and **10**, **11**, and **13** in good yield. For **6–9**, the desired stereochemistry was achieved by substituting the ethanolamine respectively with (*R*)-1-aminopropan-2-ol, (*S*)-1-aminopropan-2-ol, (*S*)-2-aminopropan-1-ol, or (*R*)-2-aminopropan-1-ol to attain cyclization with the desired pre-installed stereochemistry. Compounds **3**, **5**, and **13** were also prepared using the same cyclization method, but with ethane-1,2-diamine, 2-aminoethane-1-thiol, or 3-aminopropan-1-ol, respectively, instead of ethanolamine. As an alternative method for oxazoline cyclization, when the requisite benzonitrile was unavailable, a pre-functionalized salicylic acid was used as the basis to generate an ethanolamine-amide moiety. This ethanolamine-amide was then cyclized in the presence of thionyl chloride to form the desired oxazoline in **12** and **14–16**.

Representative data and IC_{50} value determinations are found in Figures S2-S14. Of the prepared compounds, **16** had the best activity with an IC_{50} value of 102±17 μM (Figure S12). Compounds **9**, **18**, and **13** all displayed <10% inhibition at 100 μM (Figure S14). Both **15** and **18** were found to be insoluble at concentrations >250 μM with 2.5 v/v% DMSO present in the assay buffer, preventing determination of accurate percent inhibition. Compound **5** showed no inhibition at a concentration of 100 μM. Based on this SAR, an additional inhibitor, **17**, was synthesized in a fragment merge strategy to combine the molecular features that appear to enhance potency. Combining the 2-naphthol in **16** with the imidazoline **3** resulted in **17** with an IC_{50} value of 31±1 μM, the best among the molecules prepared in this study (Figure S13).

Discussion

The use of MBPs to discover new, metal-binding metalloenzyme inhibitors has been a fruitful strategy, and has been employed against a variety of metalloenzyme targets, including glyoxalase-1, New Delhi metallo-β-lactamase-1, influenza PA_N endonuclease, proteasomal deubiquitinase Rpn11, MMP-12, and hCAII.[10,13] These MBPs produce metalloenzyme inhibition by coordinating the metal ions within the enzyme active site, thereby blocking catalysis.[10,13] Here we combine this MBP fragment library with a recently developed sensitive, real-time, fluorescence-based assay, in an effort to identify new motifs that can serve as scaffolds for new ADA inhibitors.

The key to this screening campaign was the use of an emissive adenosine surrogate (^{tz}A, Figure 1), which is effectively deaminated by ADA to the corresponding emissive inosine derivative.[8] ^{tz}A was previously found to have a similar K_M and k_{cat} to native adenosine.[7e] Its conversion to ^{tz}I can be observed by fluorescence upon excitation in the near UV wavelength range, a range typically outside the absorption spectra of the native nucleosides and simple pharmacophores. Taking advantage of the emissive properties of ^{tz}A and its similar reaction time to adenosine, we were able to translate this enzymatic assay to a more useful HTS format using standard plate readers. To validate the HTS format and methods used, EHNA, a known ADA inhibitor, was assessed and found to have an IC_{50}=6 nM, consistent with previously reported values (Figure S1).[1a,7d,e] One of the more potent fragments identified in the screen, **3** was found to have an IC_{50}=93 μM, providing an excellent starting point for additional study (Figure S3).

To preliminarily establish SAR, two of the fragments, **3** and **4**, were used as core scaffolds for inhibitor exploration. Although **3** was more active against ADA than **4**, the oxazoline scaffold was selected for preliminary SAR study, as it was more amenable towards derivatization. A cursory SAR exploration of **4**, with the intent of applying discovered trends towards the more active scaffold **3**, was performed. As such, eleven compounds were synthesized, which included modifications probing for interactions with hydrophobic or hydrophilic pockets (Figure 3). For these prepared compounds, an initial screen at 100 μM was performed to provide preliminary insight into the most active modifications. Compounds that showed <10% inhibition at 100 μM were not further analyzed. The remaining compounds were then screened at various concentrations to derive IC_{50} values, as described in the experimental section.

The SAR study indicated a methyl group at the 4 position of the dihydro-oxazole ring in **6** and **7** slightly increased potency. However, incorporation of a methyl substituent at the 3 position of the oxazoline ring in **8** and **9** resulted in a loss of activity. Expansion of the oxazoline ring to the corresponding dihydrooxazine derivative **13** also caused a significant decrease in potency, possibly due to a disruption of the binding angle necessary for metal coordination. Additionally, incorporation of a methyl group to the aromatic ring in **10**, **11**, and **12** also decreased activity. Conversely, replacement of the phenol ring with an α-naphthol at the 2-position in **16** resulted in a greater than two-fold increase in potency compared to parent compound **4**. Whereas replacement with a β-naphthol attached at the 1-position in **15** had little to no effect on activity, potentially indicating a selectivity for preferred location of lipophilic bulk. Finally, altering the heteroatoms had a significant impact on inhibitor potency in that replacing the oxazoline ring in **4** with the imidazoline in **3** caused an increase in inhibition activity. A possible explanation for this increase in potency could be that the imidazoline ring serves as a better substrate mimetic of the native purine than oxazoline.

The results described above suggested that substitution of an oxazoline with an imidazoline ring and replacing the phenol with the fused aromatic derivatives such as naphthols would result in a fragment with enhanced potency. As a result, fragment **17** was synthesized and found to have an IC_{50} value of 31±1 μM (K_i = 26 ± 1 μM), the most potent inhibitor among the molecules studied here (Table 1 and Figure S13).

Conclusion

A rapid and simple HTS format for ADA inhibitors has been established using ^{tz}A, an emissive and isofunctional adenosine surrogate. A library of ~350 MBPs were screened using this fluorescence-based assay in a 96-well plate format. Among them, 36 compounds inhibiting ADA by more than 50% at 200 μM were discovered. To generate some SAR, 11 derivatives were synthesized and analyzed. This focused collection, shedding light on the molecular features that contribute to inhibitory activity, has guided the synthesis of a merged molecule with the highest potency among these MBP fragments. Future work in this study will entail use of this fluorescent HTS assay to guide rational elaboration of **17** to attain more potent ADA inhibitors. Importantly, we are unaware of a metal-centric approach for the development of ADA inhibitors. It is possible that MBP-based inhibitors could open up new avenues for medicinal chemistry that have not yet been explored by prior ADA inhibitor classes.

Experimental Section

Unless otherwise noted, reagents were purchased from commercially available sources, and were used with no additional purification. Solvents were purchased from Sigma-Aldrich and Fisher Scientific, and dried by standard techniques. Silica gel column chromatography was performed using either a CombiFlash Rf or Rf$^+$ Teledyne ISCO system, using hexane, ethyl acetate, CH_2Cl_2 or MeOH as eluents. Separations were monitored via UV absorbance, reading at 250 and 280 nm, as well as by a Teledyne ISCO RF$^+$ PurIon ESI-MS detector with 1 Da resolution. ^{1}H and ^{13}C NMR spectra were obtained using either a Varian 400

MHz or a Varian 500 MHz spectrometer at the Department of Chemistry and Biochemistry at UC San Diego. NMR data is reported in parts per million relative to the residual non-deuterated solvent signals. When available, coupling constants (*J*) are reported in hertz (Hz). Standard resolution mass spectrometry was performed at either the UC San Diego Molecular Mass Spectrometry Facility or on the previously described Teledyne ISCO RF^+ PurIon ESI-MS detector. Analytical HPLC and high-resolution mass spectrometry using an ESI-TOF probe were performed at the UC San Diego Molecular Mass Spectrometry Facility.

Synthesis

^{tz}A was synthesized based on previously published procedures.[8] Compound **18** was purchased from Matrix Scientific. Compound **1** was prepared as previously reported.[13f] Lead compound **17** was prepared following the exact protocol as reported in Sapegin, A. et. al.[14] and matched all literature characterization. Experimental ^{1}H and ^{13}C NMR for all prepared compounds are reported in the Supplementary Information (Figure S15-S30). The purity of **3–17** was determined to be at least 97% by analytical HPLC (Figures S31-S45).

General Method for Oxazoline Derivative Synthesis

General Method for Oxazoline Cyclization: To a solution of 2-nitrilephenol (1 eq.) in toluene (5 mL), $ZnCl_2$ (0.02 eq.) and aminoethanol (1.5 eq.) were sequentially added. The mixture was purged with nitrogen and heated to reflux at 130°C for 20 h. After cooling to RT, the reaction was concentrated under reduced pressure and the residue was taken up in water and ethyl acetate. The aqueous phase was extracted with ethyl acetate (5×5 mL), the combined organic phase was dried over magnesium sulfate, and the filtrate was concentrated under reduced pressure. The resulting pink-brown residue was purified by column chromatography with a gradient of 0% to 20% ethyl acetate in hexanes, unless otherwise noted. Desired fractions were combined and concentrated under reduced pressure to obtain the desired oxazoline derivative. Compounds that were isolated as oils were cooled to −20°C for 1 h to solidify, and remained solid thereafter.

(*S*)-2-(5-Methyl-4,5-dihydrooxazol-2-yl)phenol (6): From the general method for oxazoline cyclization, from 2-hydroxybenzonitrile (0.500 g, 4.20 mmol), $ZnCl_2$ (11.4 mg, 83.9 μmol), and (S)-1-aminopropan-2-ol (473 mg, 6.30 mmol) in toluene (5 mL) at 130°C for 20 h, the desired product **6** (0.270 g, 1.52 mmol, 36%) was obtained as a clear oil that solidified upon cooling to −20°C to a white crystalline solid. ^{1}H NMR (400 MHz, DMSO-d_6): δ 12.28 (*br* s, 1H), 7.60 (d, *J*=8.0, 1H), 7.41 (t, *J*=7.2, 1H), 6.96 (d, *J*=8.4, 1H), 6.90 (t, *J*=7.6, 1H), 4.97–4.87 (m, 1H), 4.17 (ddd, J_1=14.4, J_2=9.6, J_3=2.8, 1H), 3.61 (ddd, J_1=14.4, J_2=7.6, J_3=2.8, 1H), 2.49 (d, *J*=1.6, 3H); ^{13}C NMR (500 MHz, DMSO-d_6): δ 165.2, 159.6, 134.0, 128.2, 119.3, 116.9, 110.7, 76.4, 59.6, 21.0; HRMS (ESI-TOF): *m/z* calcd for $C_{10}H_{12}NO_2$+H^+: 178.0863 $[M+H]^+$; found: 178.0864.

(R)-2-(5-Methyl-4,5-dihydrooxazol-2-yl)phenol (7): From the general method for oxazoline cyclization, from 2-hydroxybenzonitrile (0.500 g, 4.20 mmol), $ZnCl_2$ (11.4 mg, 83.9 μmol), and (R)-1-aminopropan-2-ol (473 mg, 6.30 mmol) in toluene (5 mL) at 130°C for 20 h, the desired product **7** (0.440 g, 2.48 mmol, 59%) was obtained as a clear oil that solidified upon cooling to −20°C to a white crystalline solid. ^{1}H NMR (400 MHz, DMSO-

d_6): δ 12.28 (*br* s, 1H), 7.59 (d, J=8.0, 1H), 7.41 (t, J=7.6, 1H), 6.96 (d, J=8.0, 1H), 6.90 (t, J=8.0, 1H), 4.97–4.88 (m, 1H), 4.16 (dd, J_1=14.0, J_2=9.6, 1H), 3.61 (dd, J_1=14.4, J_2=7.6, 1H), 1.37 (d, J=6.4, 3H); ^{13}C NMR (500 MHz, DMSO-d_6): δ 165.2, 159.6, 134.0, 128.2, 119.3, 116.9, 110.7, 76.4, 59.6, 21.0; HRMS (ESI-TOF): *m/z* calcd for $C_{10}H_{12}NO_2$+H^+: 178.0863 $[M+H]^+$; found: 178.0864.

General Method for High Throughput Screen

For all assay screening, bovine spleen ADA was used, as it has 91% sequence similarity overall with human ADA, and is highly conserved at the active site.[15] Therefore, the values obtained with bovine spleen ADA should be comparable with human ADA. Concentrated stock solutions were prepared for ^{tz}A (8.4 mM) and potential inhibitors (50 mM) in DMSO. Bovine spleen ADA was obtained from Sigma Aldrich (EC Number 232-817-5). The commercial suspension (1150 UmL^{-1} in 3.2 M $(NH_4)_2SO_4$, 0.01 M potassium phosphate, pH 6.0) was diluted to 1.15 UmL^{-1} by dissolving an aliquot (1 μL) in freshly prepared phosphate buffer (999 μL, 50 mM, pH 7.4). A freshly prepared enzyme stock solution was kept on ice prior to use. Fresh dilutions of ^{tz}A (7.8 μM) and enzyme (13.8 $mUmL^{-1}$) in previously prepared phosphate buffer were made just before the reaction and kept at room temperature. All high throughput assays were run on a BioTek Synergy H4 microplate reader. Reactions were run in Costar black 96-well plates that were filled and then inserted into the plate reader. Temperature was maintained at 37.0±0.1 °C. Reagents and enzymes were added in the following order: 20 μL of inhibitor first, 30 μL of enzyme second, and 50 μL of ^{tz}A last. Wells were excited at 322 nm and emission monitored at 410 nm. Intensity of emission was measured every 37 seconds for just over 30 minutes.

High Throughput Screen of EHNA

Fresh dilutions of EHNA (0.05, 0.5, 5, 12.5, 50, 125, 500, 1250, 5000, 50000 nM) in phosphate buffer were prepared. ADA (30 μL of 13.8 $mUmL^{-1}$ solution) and EHNA (20 μL) were added to successive wells in a row and thoroughly mixed. Phosphate buffer was used as a negative control. Two more rows were prepared in the same manner and a fourth row was prepared with phosphate buffer in place of ADA. After two minutes of incubation, ^{tz}A (50 μL of 7.8 μM) was added and mixed thoroughly. Wells were then excited at 322 nm and emission monitored at 410 nm. Intensity of emission was measured every 37 seconds for just over 30 minutes.

High Throughput Screen of MBP Library

Fresh dilutions of each inhibitor (1 mM) in phosphate buffer were prepared. 30 μL of 13.8 $mUmL^{-1}$ ADA and 20 μL of each inhibitor were added to successive wells in a row and thoroughly mixed. In the final two wells of the row, phosphate buffer and EHNA were added, respectively, in place of inhibitor. Two more rows were prepared in the same manner and a fourth row was prepared with phosphate buffer in place of ADA. After two minutes of incubation, ^{tz}A (50 μL of 7.8 μM) was added and mixed thoroughly. Wells were then excited at 322 nm and emission monitored at 410 nm. Intensity of emission was measured every 37 seconds for just over 30 minutes.

IC_{50} Analysis of 2

Fresh dilutions of **2** (0.005, 0.05, 0.125, 0.5, 5, 12.5, 50, 125, 500, 1000 μM) in phosphate buffer were prepared. 30 μL of 13.8 $mUmL^{-1}$ ADA and 20 μL of **2** were added to successive wells in a row and thoroughly mixed. In the final two wells of the row, phosphate buffer and EHNA were added, respectively, in place of **2**. Two more rows were prepared in the same manner and a fourth row was prepared with phosphate buffer in place of ADA. After two minutes of incubation, ^{tz}A (50 μL of 7.8 μM) was added and mixed thoroughly. Wells were then excited at 322 nm and emission monitored at 410 nm. Intensity of emission was measured every 37 seconds for just over 30 minutes.

IC_{50} Analysis of 4 and Derivatives

Concentrated stock solutions were prepared for ^{tz}A (1 mM) and potential inhibitors (100 mM) in DMSO. Bovine spleen ADA was obtained from Sigma Aldrich (EC Number 232-817-5). The commercial solution was diluted to 1.15 UmL^{-1} by dissolving an aliquot (1 μL) in freshly prepared phosphate buffer (999 μL, 50 mM, pH 7.4). The enzyme stock solution was freshly prepared and kept on ice prior to use. Fresh dilutions of each compound tested were prepared (1, 10 mM) in DMSO from the 100 mM stock solution. For **17**, an additional 0.1 mM solution in DMSO was prepared. Emission change was monitored on a Horiba Fluoromax-4 equipped with a cuvette holder with a stirring system setting both the excitation and the emission slits at 3 nm, the resolution at 1 nm and the integration time 0.1 s. The Horiba Fluoromax-4 was equipped with a thermostat controlled ethylene glycol-water bath fitted to specially designed cuvette holder and the temperature was kept at 25.0±0.1 °C. Reactions were monitored in a 3 mL quartz cuvette while stirring. 1.7 mL of phosphate buffer was added to the cuvette. A volume equal to the sum of the ^{tz}A, ADA, and compound volumes was removed from the cuvette. If the final concentration of inhibitor was 10, 100, or 1000 μM, 17 μL of 1, 10, or 100 mM compound solution was added, respectively. If the final concentration of inhibitor was 1 μM, 1.7 μL of 1 mM **4** derivative solution was added. If the final concentration of inhibitor was 25 or 250 μM, 4.25 μL of 10 or 100 mM **4** derivative solution was added, respectively. For a final concentration of 0.1 μM **17**, 1.7 μL of 0.1 mM solution was added. 6.6 μL of ^{tz}A was added to the cuvette and the solution was stirred for 1 minute. Initial emission at 410 nm upon excitation at 322 nm was measured. ADA was added and measurements continued every 10 seconds for 20 minutes.

Note: For fragments **14**, **15**, and **16** at concentrations of 25 and 250 μM, 42.5 μL of 1 and 10 mM were added, respectively.

Data Analysis

The signal intensity of each time point of ^{tz}A conversion to ^{tz}I was converted to a percent change relative to the initial intensity. The corresponding percent change values of the run without ADA were then subtracted from the runs with inhibitor. The final point of each curve was then divided by the final point of the run without inhibitor to yield the percent activity for that run. The percent activity of each inhibitor concentration was then subtracted from one to yield the percent inhibition. For IC_{50} value determination, percent inhibition points were plotted against the respective inhibitor concentration on a logarithmic scale x-

axis. The resulting plot was fit with a Hill curve and the IC_{50} value calculated from the constants. IC_{50} values were converted to K_I values using the Cheng-Prusoff equation.

Supplementary Material

Refer to Web version on PubMed Central for supplementary material.

Acknowledgements

The authors would like to thank Dr. Yongxuan Su for mass spectrometry sample analysis at the UC San Diego Chemistry and Biochemistry Mass Spectrometry Facility. We also thank the remaining members of the Cohen and Tor Laboratory groups, both former and current, for their support and advice; in particular Dr. Cy Credille for preparing compound **2**. This work was supported by National Institute of Health grant R01 GM098435, R01 AI149444, R01 GM069773, and the Chemical Biology Interfaces at UC San Diego training grant T32GM112584-01. S.M.C. is a cofounder of and has an equity interest in Cleave Therapeutics and Forge Therapeutics, companies that may potentially benefit from the research results. S.M.C. also serves on the Scientific Advisory Board for these companies. The terms of this arrangement have been reviewed and approved by the University of California, San Diego in accordance with its conflict of interest policies.

References

[1]. a)Cristalli G, Costanzi S, Lambertucci C, Lupidi G, Vittori S, Volpini R, Camaioni E, Med. Res. Rev 2001, 21, 105–128 [PubMed: 11223861] b)Tardif V, Muir R, Cubas R, Chakhtoura M, Wilkinson P, Metcalf T, Herro R, Haddad EK, Nat. Commun 2019, 10, 823. [PubMed: 30778076]

[2]. a)Nakajima Y, Kanno T, Nagaya T, Kuribayashi K, Nakano T, Gotoh A, Nishizaki T, Cell. Physiol. Biochem 2015, 35, 51–60 [PubMed: 25547995] b)Kutryb-Zajac B, Koszalka P, Mierzejewska P, Bulinska A, Zabielska MA, Brodzik K, Skrzypkowska A, Zelazek L, Pelikant-Malecka I, Slominska EM, Smolenski RT, J. Cell. Mol. Med 2018, 22, 5939–5954. [PubMed: 30291675]

[3]. a)Sauer AV, Brigida I, Carriglio N, Aiuti A, Front. Immunol 2012, 3, 265 [PubMed: 22969765] b)Mediero A, Cronstein BN, Trends Endocrinol. Metab 2013, 24, 290–300 [PubMed: 23499155] c)Kutryb-Zajac B, Mateuszuk L, Zukowska P, Jasztal A, Zabielska MA, Toczek M, Jablonska P, Zakrzewska A, Sitek B, Rogowski J, Lango R, Slominska EM, Chlopicki S, Smolenski RT, Cardiovasc. Res 2016, 112, 590–605 [PubMed: 28513806] d)Cortes A, Gracia E, Moreno E, Mallol J, Lluis C, Canela EI, Casado V, Med. Res. Rev 2015, 35, 85–125 [PubMed: 24933472] e)Antonioli L, Csoka B, Fornai M, Colucci R, Kokai E, Blandizzi C, Flasko G, Drug Discovery Today 2014, 19, 1051–1068 [PubMed: 24607729] f)Antonioli L, Colucci R, La Motta C, Tuccori M, Awwad O, Da Settimo F, Blandizzi C, Fornai M, Curr. Drug Targets 2012, 13, 842–862. [PubMed: 22250650]

[4]. a)Schaeffer FIJ, Schwender CF, J. Med. Chem 1974, 17, 6–8 [PubMed: 4808472] b)Gillerman I, Fischer B, J. Med. Chem 2011, 54, 107–121. [PubMed: 21138280]

[5]. a)McConnell WR, El Dareer SM, Hill DL, Drug Metab. Dispos 1980, 8, 5–7 [PubMed: 6102030] b)Lambe CU, Nelson DJ, Biochem. Pharmacol 1982, 31, 535–539. [PubMed: 7066021]

[6]. a)Zimmermann SC, Sadler JM, O'Daniel PI, Kim NT, Seley-Radtke KL, Nucleosides Nucleotides Nucleic Acids 2013, 32, 137–154 [PubMed: 23473101] b)Tite T, Lougiakis N, Myrianthopoulos V, Marakos P, Mikros E, Pouli N, Tenta R, Fragopoulou E, Nomikos T, Tetrahedron 2010, 66, 9620–9628c)Li G, Nakagome I, Hirono S, Itoh T, Fujiwara R, Pharmacol. Res. Perspect 2015, 3, e00121 [PubMed: 26038697] d)Da Settimo F, Primofiore G, La Motta C, Taliani S, Simorini F, Marini AM, Mugnaini L, Lavecchia A, Novellino E, Tuscano D, Martini C, J. Med. Chem 2005, 48, 5162–5174. [PubMed: 16078836]

[7]. a)Zhang L, Zhao J, Jiang J, Yu R, Chem. Commun. (Camb.) 2012, 48, 10996–10998 [PubMed: 23037591] b)Xu Y, Venton BJ, Phys. Chem. Chem. Phys 2010, 12, 10027–10032 [PubMed: 20577678] c)Xing XJ, Liu XG, Yue H, Luo QY, Tang HW, Pang DW, Biosens. Bioelectron 2012, 37, 61–67 [PubMed: 22613226] d)Sinkeldam RW, McCoy LS, Shin D, Tor Y, Angew. Chem. int. Ed. Engl 2013, 52, 14026–14030 [PubMed: 24288262] e)Ludford PT 3rd, Rovira AR, Fin A, Tor

Y, ChemBioChem 2019, 20, 718–726 [PubMed: 30566279] f)Hu K, Huang Y, Wang S, Zhao S, J. Pharm. Biomed. Anal 2014, 95, 164–168. [PubMed: 24682016]

[8]. Rovira AR, Fin A, Tor Y, J. Am. Chem. Soc 2015, 137, 14602–14605. [PubMed: 26523462]

[9]. a)Wilson DK, Quiocho FA, Biochemistry 1993, 32, 1689–1694 [PubMed: 8439534] b)Wilson DK, Rudolph FB, Quiocho FA, Science 1991, 252, 1278–1284. [PubMed: 1925539]

[10]. Chen AY, Adamek RN, Dick BL, Credille CV, Morrison CN, Cohen SM, Chem. Rev 2019, 119, 1323–1455. [PubMed: 30192523]

[11]. Yang Y, Hu XQ, Li QS, Zhang XX, Ruan BF, Xu J, Liao C, Curr. Top. Med. Chem 2016, 16, 384–396. [PubMed: 26268345]

[12]. a)Bergeron RJ, Chem. Rev 1984, 84, 587–602b)Hoveyda HR, Karunaratne V, Rettig SJ, Orvig C, Inorg. Chem 1992, 31, 5408–5416.

[13]. a)Perez C, Barkley-Levenson AM, Dick BL, Glatt PF, Martinez Y, Siegel D, Momper JD, Palmer AA, Cohen SM, J. Med. Chem 2019, 62, 1609–1625 [PubMed: 30628789] b)Li J, Zhang Y, Da Silva Sil Dos Santos B, Wang F, Ma Y, Perez C, Yang Y, Peng J, Cohen SM, Chou TF, Hilton ST, Deshaies RJ, Cell Chem. Biol 2018, 25, 1350–1358 e1359 [PubMed: 30146242] c)Credille CV, Dick BL, Morrison CN, Stokes RW, Adamek RN, Wu NC, Wilson IA, Cohen SM, J. Med. Chem 2018, 61, 10206–10217 [PubMed: 30351002] d)Chen AY, Thomas PW, Stewart AC, Bergstrom A, Cheng Z, Miller C, Bethel CR, Marshall SH, Credille CV, Riley CL, Page RC, Bonomo RA, Crowder MW, Tierney DL, Fast W, Cohen SM, J. Med. Chem 2017, 60, 7267–7283 [PubMed: 28809565] e)Chen AY, Thomas PW, Cheng Z, Xu NY, Tierney DL, Crowder MW, Fast W, Cohen SM, ChemMedChem 2019, 14, 1271–1282 [PubMed: 31124602] f)Adamek RN, Credille CV, Dick BL, Cohen SM, J. Biol. Inorg. Chem 2018, 23,1129–1138. [PubMed: 30003339]

[14]. Sapegin A, Osipyan A, Krasavin M, Org. Biomol. Chem 2017, 15, 2906–2909. [PubMed: 28321443]

[15]. Kinoshita T, Nishio N, Sato A, Murata M, Acta Crystallogr. Sect. D 1999, 55, 2031–2032. [PubMed: 10666580]

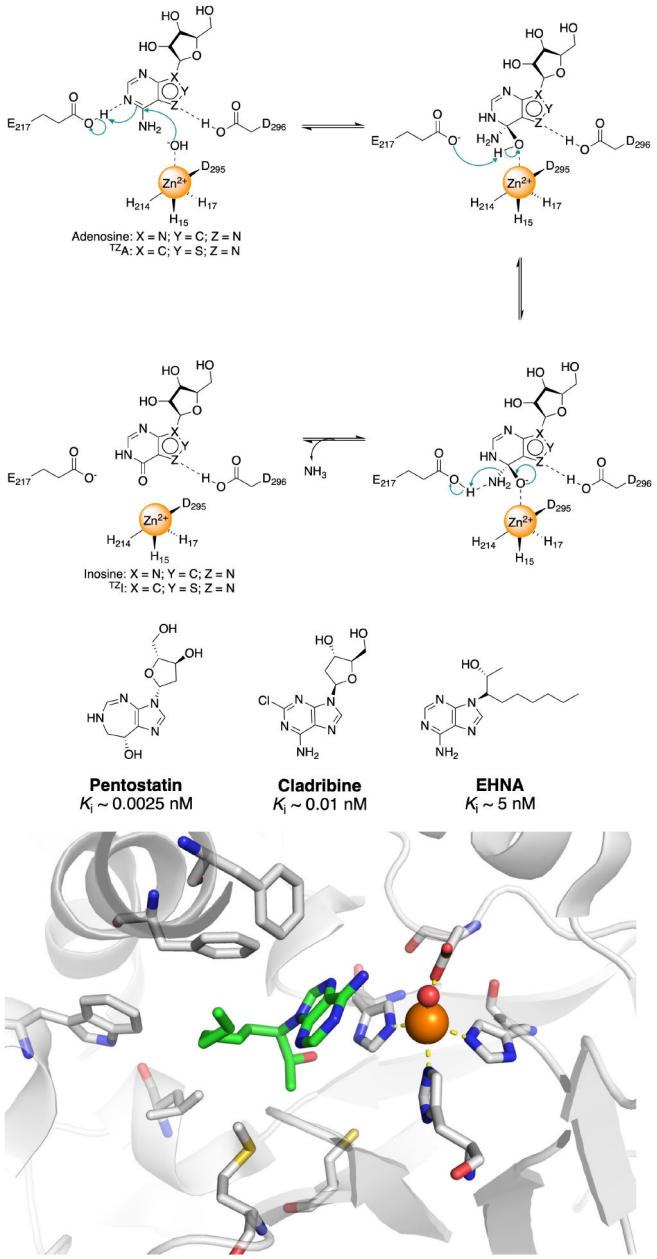

Figure 1.

Top: Mechanistic depiction of ADA-mediated deamination of adenosine as well as ^{tz}A deamination to yield the active fluorophore *^{tz}I*. Middle: Structure and K_i values of ADA inhibitors Pentostatin, Cladribine, and EHNA. Bottom: Crystal structure of EHNA (green) bound to the ADA active site (PDB ID: 2Z7G). Key residues, catalytic Zn^{2+} (orange sphere), and Zn^{2+}-bound water (red sphere) are highlighted.

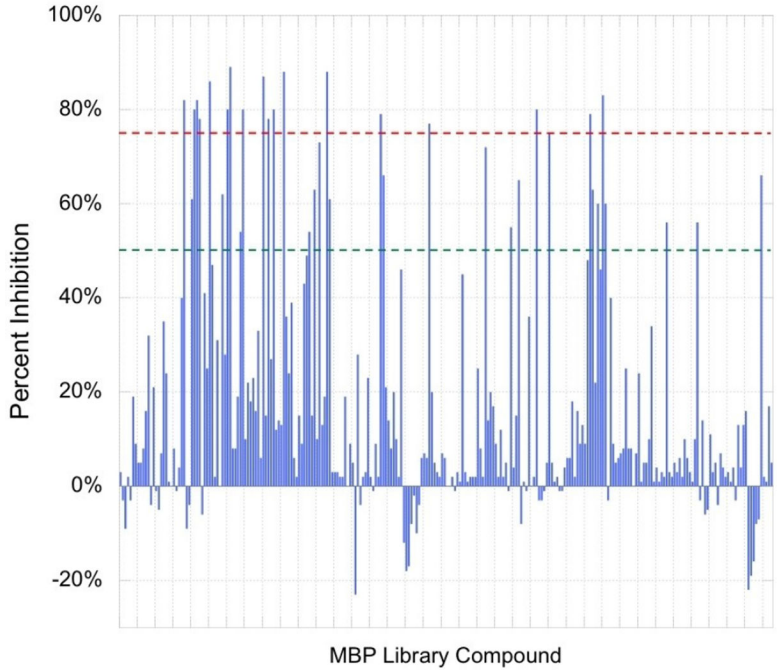

Figure 2.

Results of the MBP library screen against ADA, represented as a bar graph of percent inhibition (relative to no inhibitor) of ADA in the presence of 200 μM MBP fragment. The green dashed line denotes compounds with greater than 50% inhibition, and the red dashed line denotes compounds with greater than 75% inhibition.

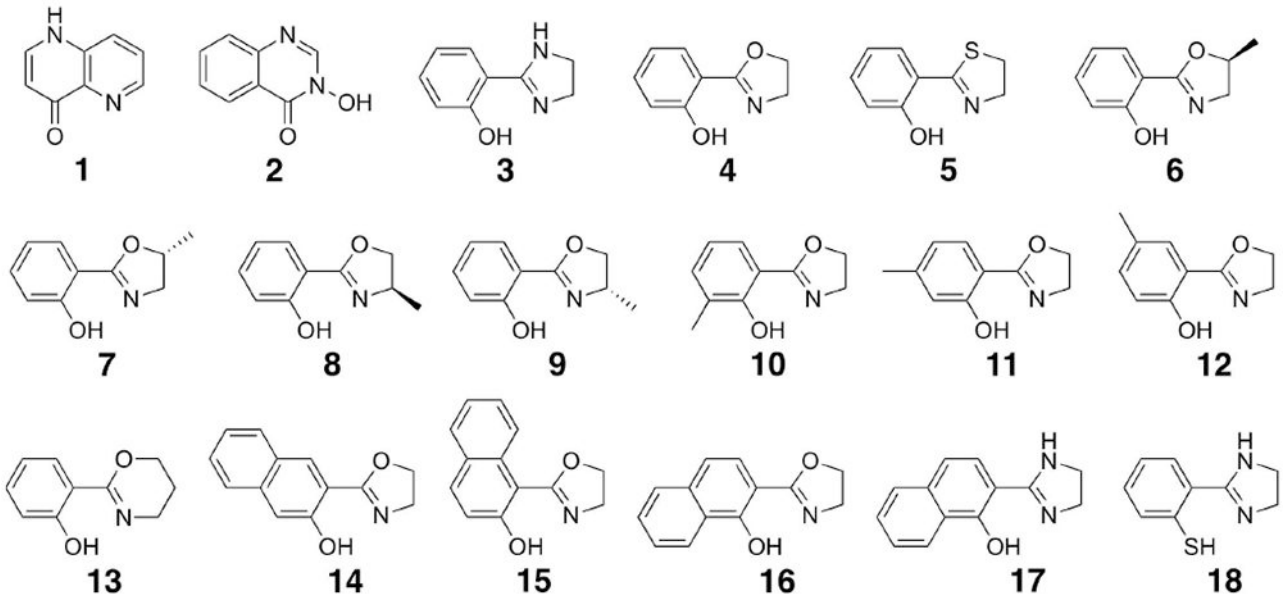

Figure 3.
MBP compounds tested against ADA in this study.

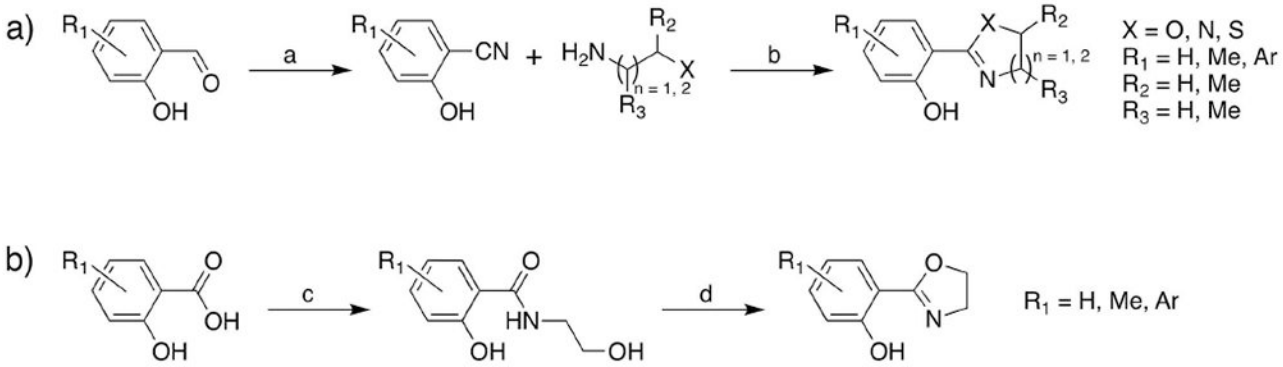

Scheme 1.

General method for oxazoline synthesis by: a) cyclization reaction between ethanolamine or aminopropanol with an aromatic nitrile or b) by cyclizing amide-coupled ethanolamine. Reagents and conditions: (a) potassium acetate, hydroxylamine hydrochloride, formic acid, 100°C, 24 h, 57% yield; (b) $ZnCl_2$, ethanolamine, toluene, 130°C, 24 h, 75% yield; (c) ethanolamine, triethylamine, T3P, tetrahydrofuran, ethyl acetate, 70°C, 16 h, 24% yield; (d) EDC, HOBt, triethylamine, ethanolamine, DMF, 60°C, 16 h, 20% yield.

Table 1.

IC_{50} and K_i Values of prepared oxazoline derivatives. Standard deviations listed are calculated from three independent experiments.

Compound	IC_{50} [μM]	K_i [μM]
EHNA	0.006±0.002[a]	0.005±0.002[a]
	0.023±0.004[b]	0.019±0.004[b]
		~0.005[c]
Pentostatin	0.0014±0.0001[b]	0.0012±0.0002[b]
3	93±17	77±14
4	260±14	215±12
5	>700	n.d.
6	194±4	161±3
7	188±10	156±8
8	455±8	377±7
9	>700	n.d.
10	>700	n.d.
11	618±9	512±7
12	372±24	308±20
13	>700	n.d.
14	Insoluble	Insoluble
15	273±19	226±15
16	102±17	85±14
17	31±1	26±1
18	Insoluble	Insoluble

[a] Values were determined using the HTS assay format reported here (Figure S1)

[b] Values determined using a non-HTS assay format[8e]

[c] Value reported in Cristalli et al.[1a]